

Strong terahertz response in bilayer graphene nanoribbons

A. R. Wright,¹ J. C. Cao,² and C. Zhang^{(a)1}

¹*School of Engineering Physics, University of Wollongong, New South Wales 2552, Australia*

²*State Key Laboratory of Functional Materials for Informatics,
Shanghai Institute of Microsystem and Information Technology,
Chinese Academy of Sciences, 865 Changning Road, Shanghai 200050, P. R. China*

We reveal that there exists a class of graphene structures (a sub-class of bilayer graphene nanoribbons) which has unusually strong optical response in the terahertz (THz) and far infrared (FIR) regime. The peak conductance of terahertz/FIR active bilayer ribbons is around two orders of magnitude higher than the universal conductance of $e^2/4\hbar$ observed in graphene sheets. The criterion for the terahertz/FIR active sub-class is a bilayer graphene nanoribbon with one-dimensional massless Dirac Fermion energy dispersion near the Γ point. Our results overcome a significant obstacle that hinders potential application of graphene in electronics and photonics.

PACS numbers: 73.50.Mx, 78.67.-n, 81.05.Uw

In recent years, graphene has attracted a great deal of interest[1, 2, 3, 4]. New physics have been predicted and observed, such as electron-hole symmetry and half-integer quantum Hall effect[2, 3], finite conductivity at zero charge-carrier concentration[2], and the strong suppression of weak localization[5, 6, 7]. Bilayer graphene (BLG) has also attracted considerable attention recently, with seminal experimental and theoretical work being carried out [1, 8]. Bilayer calculations use interlayer coupling constants based on the Slonczewski-Weiss-McClure model [9, 10]. By further confining the electrons in the graphene plane, one can obtain one-dimensional structures which we refer to as graphene nanoribbons (GNRs)[11]. It has been shown that GNRs with zigzag edges can have finite magnetization with either ferromagnetic order or antiferromagnetic order[12, 13]. These properties promise building blocks for technological applications in molecular electronic and optoelectronic devices.

The optical properties of graphene systems is a topic of considerable interest. In particular, the minimal conductivity of single layer graphene (SLG) within the Dirac regime is a much celebrated result which was calculated theoretically long before graphene's fabrication in 2003 [14]. The optical conductivity of SLG outside the low energy Dirac regime has been calculated theoretically[15, 16]. The conductance of bilayer graphene has also been calculated [17], as has the conductance of various GNRs [18]. All of this research has shown that the optical responses of graphene and graphene nanoribbons are extremely weak. In the EM frequency band from terahertz to visible, the absorption coefficient for these systems is generally less than 3%. [19, 20, 21]. While the lateral confinement and the edge states can lead to the ferromagnetic and antiferromagnetic order in GNRs[12], the optical response of all ribbons remains very weak. There are two fundamental reasons for this: (1) the density of states vanishes near the Fermi energy, and (2) the interband transition am-

plitude is small. Because of this, potential application of graphene structures in optoelectronics and photonics is severely limited. To date, these obstacles have remained.

However we are now able to demonstrate that there exists a sub-class of bilayer graphene nanoribbons (BLGNRs) which have an unusually strong optical conductance in the terahertz (THz) to far infrared (FIR) regime. The height of the conductance peak is close to two orders of magnitude greater than the universal conductance of graphene sheets. We found that this sub-class of BLGNRs can be either armchair or chiral, but their energy dispersion near the Γ point must be that of a one-dimensional massless Dirac Fermion. This sub-class of graphene structures are the first systems to show such a strong optical response in the absence of any external field in the important frequency band of THz and FIR.

We first construct a single layer GNR (SLGNR) following the convention of Ezawa [22], i.e., a ribbon is specified by two indices p and q . We begin by placing $m = p + q$ hexagons next to each other with flat edges touching. On top of this layer, we place an identical layer, offset by q hexagons. Continuing this in both directions we can construct a GNR of arbitrary chirality. Within this model $q = 0$ corresponds to a zig-zag (ZZ) edged ribbon, and $q = 1$ corresponds to an armchair (AC) edged ribbon. $q > 1$ corresponds to arbitrary chirality, defined by an angle $\theta = \tan^{-1}(\sqrt{3}/(2q + 1))$. The number of atoms in the unit cell is given by $N_u = 4q + 2p + 2$. The second layer is now constructed by assuming the standard $A - B$ 'Bernal' stacking, along the vertical $C - C$ vector. The net effect is simply shifting the entire second layer up (or down) by an amount $C - C = 1.42\text{\AA}$. A typical BLGNR is shown in Figure 1.

The intralayer coupling is calculated using the tight binding formalism where $t \approx 3eV$ is the nearest neighbour hopping integral. The edge effects of GNRs are incorporated into the tight binding formalism by setting the overlap integral to zero for hopping between edge

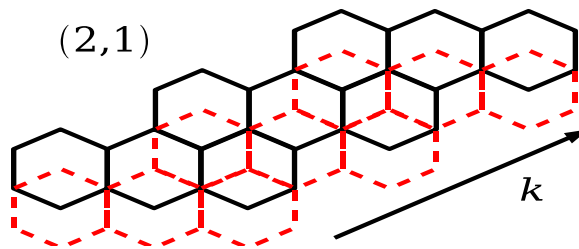


FIG. 1: The construction of a bilayer graphene nanoribbon. The second layer is identical to the first, but shifted along a C-C vector.

sites and their neighbours which are off the edge of the ribbon. In this way, the edge states are incorporated into the full electronic properties. The interlayer coupling is restricted to the dominant coupling term $\gamma = 0.36eV$ which occurs only between A and B sites which sit directly one on top of the other. As an example the Hamiltonian matrix for a (2,1) BLG NR is given by

$$H_{(2,1)} = \begin{pmatrix} H_{\text{intra}} & H_{\text{inter}} \\ H_{\text{inter}}^* & H_{\text{intra}} \end{pmatrix} \quad (1)$$

Where the intralayer terms are given by

$$H_{\text{intra}} = \begin{pmatrix} 0 & h \\ h^* & 0 \end{pmatrix} \quad (2)$$

And

$$h = \begin{pmatrix} h_1 & h_2 & 0 & 0 & 0 \\ h_1^* & h_1 & h_2 & 0 & 0 \\ 0 & h_1^* & h_1 & 0 & h_2 \\ 0 & 0 & h_1^* & h_2 & h_1 \\ 0 & 0 & 0 & h_1 & h_1^* \end{pmatrix} \quad (3)$$

Where $h_1 = e^{ikb\sqrt{3}/2}$, and $h_2 = e^{ikb}$. The interlayer coupling matrix is given by

$$H_{\text{inter}} = \begin{pmatrix} 0 & h' \\ h^{T'} & 0 \end{pmatrix} \quad (4)$$

Where

$$h' = \begin{pmatrix} 0 & \gamma & 0 & 0 & 0 \\ 0 & 0 & \gamma & 0 & 0 \\ 0 & 0 & 0 & 0 & \gamma \\ 0 & 0 & 0 & \gamma & 0 \\ 0 & 0 & 0 & 0 & 0 \end{pmatrix}. \quad (5)$$

The band structures for ZZ-BLG NRs are shown in Figure 2(a). They differ from the single layer case as the interlayer coupling produces a second subband corresponding to each single layer subband offset by an amount

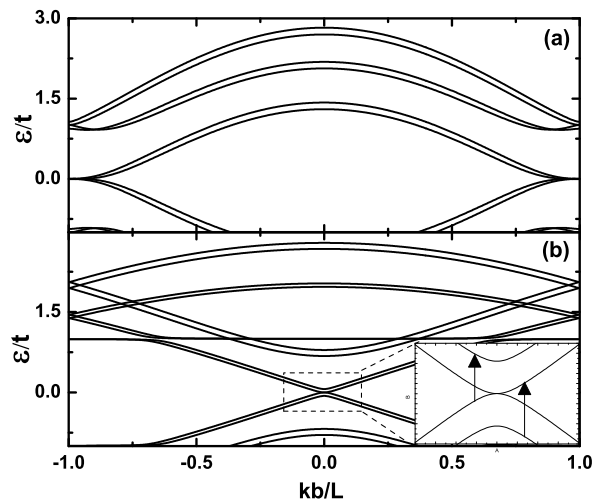


FIG. 2: The bilayer graphene nanoribbon electronic dispersion curves differ from the single layer ones as each single layer subband has a complementary subband which generally differs in energy by $< \gamma$. The zigzag case is given in (a), and the Dirac armchair case in (b). The inset to (b) shows the two sets of symmetric bands near the Dirac point. The arrow represents transitions between non-symmetric bands which is the dominant transition at low energies that leads to the unusually high optical conductance observed in figure 3(b).

γ for most of the Brillouin Zone. Near the Dirac-like points however, the intersubband gap goes to zero for the low energy bands which approach zero energy, and the higher energy bands all approach a degenerate point slightly away from the Dirac-like points. The edge states cause the plateau of the zigzag dispersion at low energies, causing an extended region of zero band-gap near the zone boundary.

The band structures of AC-BLG NRs shown in figure 2(b) behave much like 2D bilayer graphene. The linear dispersion at the Dirac points becomes curved, and a second subband appears. Each subband is thus paired. But unlike the ZZ-BLG NR case, the intersubband gap does not go to zero near the Dirac points, but remains at least $\gamma/2$ separated from it's pair. As the width increases, this gap approaches zero as the band pairs converge. This is strictly an edge effect, and in the 2D limit a band gap of γ re-emerges.

We shall show below that the oscillator strength of the interband transition is strongly dependent on the properties of the energy dispersion at the zero-gap point. We shall show below that for ZZ-BLG NR, where the zero gap position is at the K point and the two low energy dispersions are close to parabolic, the oscillator strength at low energy is very small. On the other hand, for AC-BLG NR, the zero gap position is at the Γ point. Furthermore, the two low energy dispersions are very close to linear (or a one-dimensional massless Dirac Fermion). In this case the interband transition between the bands (transitions

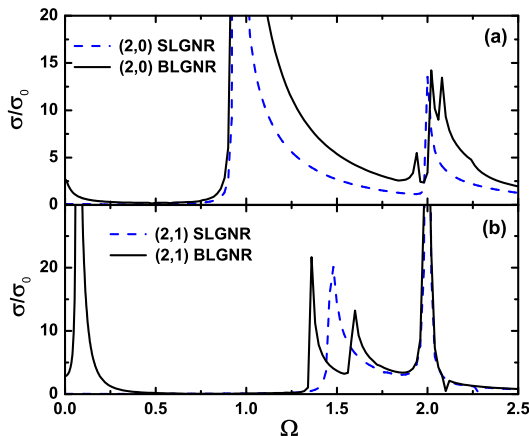


FIG. 3: The optical conductivity for the ZZ-BLGNR (a) and the AC-BLGNR (b). The low energy activity in the bilayer ribbons is particularly significant, especially in the Dirac AC-BLGNR where the optical conductivity is approximately $80\sigma_0$.

between the non-symmetric bands shown by arrows in the inset of figure 2(b)) is extremely strong.

The optical conductivity is calculated using the Kubo formula given by

$$\sigma(\omega) = \frac{1}{\omega} \int_0^\infty dt e^{i\omega t} \langle [J(t), J(0)] \rangle \quad (6)$$

Where J , the current operator is given by $\partial H/\partial y$. We define the dimensionless photon frequency $\Omega = \hbar\omega/t$, and normalize our results to the single layer universal conductivity given by $\sigma_0 = e^2/4\hbar$. We determine the dependence of the optical conductance on the ribbon widths and chiralities. In figure 3(a) we show that the optical conductivity for the ZZ-BLGNR exhibits a spike centered on zero energy. This spike occurs here because both low energy subbands approach zero energy at the Dirac-like points. In the SLGNR case, the velocity operator approaches a constant, which makes inter-symmetric-subband transitions forbidden. This is no longer the case in bilayer ribbons, and there is also now the possibility of low energy inter-non-symmetric-subband transitions.

Over the full energy spectrum, we see that some of the resonant peaks in the single layer optical conductivity spectrum have split into three peaks. This will not generally be the case. Most peaks will split into two as will be seen in the armchair case. However, near $\Omega = 1$, the subbands create a linear Dirac-like band structure with features similar to the Dirac point in the preceding armchair case, as well as those observed in 2D bilayer graphene. This means that there are three possible energy transitions with high density of states. The central, primary peak corresponds to the original SLGNR peak, and the two secondary peaks, one below, and one

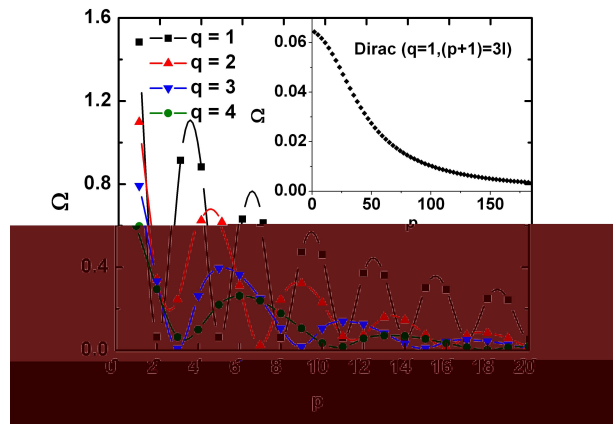


FIG. 4: The width dependence of the energy of the low-energy peak for BLGNRs with $q = [1, 4]$. The strongest peaks occur in the lowest energy gaps in the Dirac armchair ribbons. The inset shows the width dependence of the band gap for Dirac BLGNRs with strong low energy optical response. This gap eventually disappears, but in the 2D limit with no edges, it re-emerges at γ .

above the original by an amount $\Omega = \gamma$, correspond to the new curved subbands which don't quite touch the degenerate point from the single layer case.

The optical conductance of armchair BLGNRs is shown in figure 3(b), In the AC case it peaks sharply at $\gamma/2$ and trails off because of the curvature of the band structure. In the armchair case, a peak is still observed as $\Omega \rightarrow 0$, but the peak at $\gamma/2$ is about 2 orders of magnitude stronger. This peak corresponds to vertical transitions between non-symmetric subbands which are far more probable than those between symmetric ones (see fig. 5 and subsequent discussion). This single low energy peak is larger than every other peak across the spectrum. As the width of the ribbons increases, the strength of this peak decreases and the width of it broadens. In the case of an infinitely wide ribbon, the strong optical response is lost, settling at $\approx 4\sigma_0$ at $\Omega = \gamma$. This reflects the peculiar edge dependence of the bilayer ribbon system.

At higher energies, the single peaks observed in AC-SLGNRs generally have split into two, and are separated by an amount $\approx 2\gamma$. This corresponds to two sets of symmetric transitions, the non-symmetric transitions being largely suppressed.

For $q > 1$ BLGNRs, the band gap between the two lowest energy symmetric bands varies from zero to $1eV$. Similarly the non-Dirac AC-BLGNRs (ie $(p+q)/3 \notin I$), have varying band-gaps for the lowest energy subbands.

For a given type of BLGNR, the conductance peak position can be tuned with the ribbon width. Figure 4 shows the width dependence of the peak position in the THz/FIR regime. The peak position oscillates with the ribbon width. The amplitude of the oscillation is of the

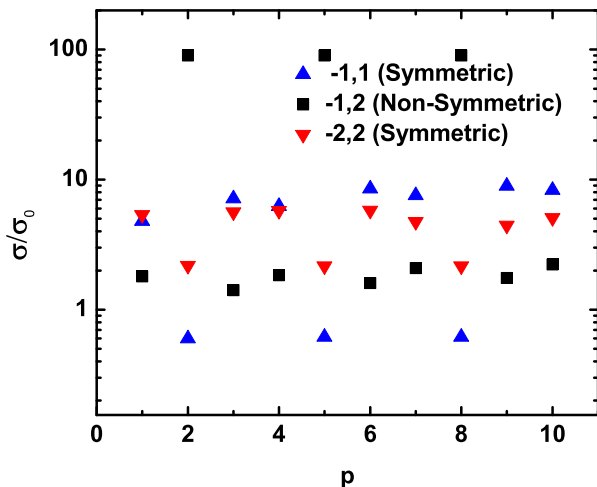


FIG. 5: The p dependence of the low energy peaks for a $(p,1)$ BLG NR. In Dirac ribbons the symmetric transitions are suppressed and the non-symmetric ones dominate. For non-Dirac ribbons the opposite is the case.

same order of magnitude as the average peak position, indicating a large range for tuning the resonance peak. The period of the oscillation increases with the chirality (q). The inset of figure 4 shows the width dependence of the energy gap for Dirac BLG NRs. This gap decreases as width increases making the location of the optical peak strongly width dependent. In the limit of infinite width this edge determined gap approaches zero, and the 2D bilayer band structure sees the emergence of a gap of γ . The optical response in this case however is not nearly so large, being $\approx 4\sigma_0$

Figure 5 shows the width dependence of the magnitude of the low energy peak for the $(p,1)$ BLG NR. For $(p+1)/3 \in I$, the non-symmetric matrix element dominates, causing the single low energy peak. The low-frequency peak conductance for this class of BLG NRs is unusually strong having a value of approximately $80\sigma_0$, much stronger than the universal conductance of graphene sheets.[21] When the Dirac condition is not met however (ie $(p+1)/3 \notin I$), the symmetric matrix elements dominate, and the non-symmetric matrix elements are greatly suppressed, leading to a much weaker response to the low energy spectrum.

The width dependence of the strength of the low energy peak for ZZ-BLG NRs is given in Figure 6. For very narrow ribbons with $p < 6$ the peak quickly decreases in magnitude at a decreasing rate. For $p > 6$ however, the peak magnitude increases steadily reflecting the low energy subband shape. As the width increases, the low energy subbands remain lower, which increases the DOS, allowing more transitions between subbands. For very narrow width ZZ-BLG NRs however, the curvature in the subbands is so high that the velocity operator allows strong coupling between the subbands, which makes the

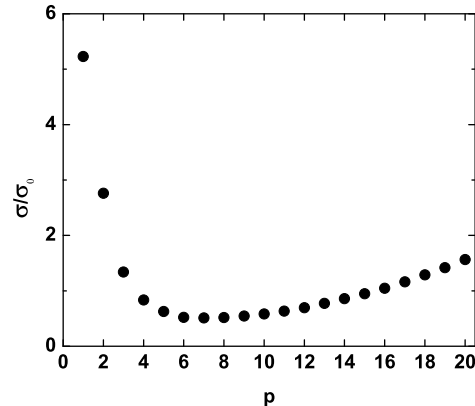


FIG. 6: The width dependence of the magnitude of the low energy peak for the ZZ-BLG NRs decreases quickly with increasing width, and then increases steadily for $p > 6$.

low energy magnitude very strong.

In summary, we have shown that the interplay of ribbon's chirality and the inter-ribbon coupling can lead to significant enhancement in optical response. We have identified a sub-class of BLG NRs where the inter-ribbon coupling causes a finite band gap in the energy minimum (maximum) and induces strong inter-subband transitions. The distinct feature of this sub-class of BLG NRs is that they have a one dimensional massless Dirac Fermion dispersion near the Γ point. The peak conductance of this class of BLG NRs has a very large value of as much as $80\sigma_0$, making them a class of materials for unique applications in optoelectronics. The simple picture behind this phenomenon is that the density of states for the 1D massless Dirac Fermions remains finite at zero energy, whereas that for the 2D massless Dirac Fermions in a graphene sheet vanishes. The peculiar role of the edge states has also been shown to contribute as the 2D limit of infinite width shows markedly decreased response in this frequency regime.

These results reported here open a gateway to the creation of graphene-based low energy photon devices. The ribbon width and chirality selection for various applications is crucial, as the optical responses of various ribbons change dramatically when these properties are varied.

Acknowledgement—This work is supported in part by the Australian Research Council.

^{a)}Electronic mail: czhang@uow.edu.au

[1] K.S. Novoselov, A.K. Geim, S.V. Morozov, D. Jiang, Y. Zhang, S.V. Dubonos, I.V. Grigorieva, A.A. Firsov, Sci-

- ence **306**, 666 (2004).
- [2] K.S. Novoselov, A.K. Geim, S.V. Morozov, D. Jiang, M.I. Katsnelson, I.V. Grigorieva, S.V. Dubonos, A.A. Firsov, Nature (London) **438**, 197 (2005).
- [3] Y. Zhang, Y.W. Tan, H.L. Stormer, P. Kim, Nature (London) **438**, 201 (2005).
- [4] C. Berger, Z. Song, X. Li, X. Wu, N. Brown, C. Naud, D. Mayou, T. Li, J. Hass, A. N. Marchenkov, E. H. Konrad, P. N. First, W. A. de Heer, Science **312**, 1191 (2006).
- [5] H. Suzuura, T. Ando, Phys. Rev. Lett. **89**, 266603 (2002).
- [6] S.V. Morozov, K.S. Novoselov, M.I. Katsnelson, F. Schedin, L.A. Ponomarenko, D. Jiang, A.K. Geim, Phys. Rev. Lett. **97**, 016801 (2006).
- [7] D.V. Khveshchenko, Phys. Rev. Lett. **97**, 36802 (2006).
- [8] E. McCann, V. I. Falko, Phys. Rev. Lett. **96** 086805 (2006).
- [9] J. C. Slonczewski, P. R. Weiss, Phys. Rev. **109**, 272 (1958).
- [10] J. W. McClure, Phys. Rev. **108**, 612 (1957).
- [11] Y. W. Son, M. L. Cohen, S. G. Louie, Phys. Rev. Lett. **97**, 216806 (2006)
- [12] Y.W Son, M. L. Cohen, S. G. Louie, Nature (London) **444**, 347 (2006)
- [13] Q. Yan, B. Huang, J. Yu, F. Zheng, J. Zang, J. Wu, B-L. Gu, F. Liu, W. Duan, Nano Letters **7** 1469 (2007).
- [14] E. Fradkin, Phys. Rev. B **33**, 3263 (1986).
- [15] C. Zhang, L. Chen, Z. Ma, Phys. Rev. B, **77** 241402 (2008).
- [16] T. Stauber, N. M. R. Peres, A. K. Geim, Phys. Rev. B, **78** 085432 (2008).
- [17] J. Cserti, A. Csordas, G. David, Phys. Rev. Lett., **99** 066802 (2007).
- [18] J. Liu, A.R. Wright, C. Zhang, Z. Ma, App. Phys. Lett., **93**, 041106 (2008).
- [19] V.P. Gusynin, S.G. Shrapov, J.P. Carbotte, Phys. Rev. Lett. **96**, 56802 (2006).
- [20] A. B. Kuzmenko, E. van Heumen, F. Carbone, D. van der Marel, Phys. Rev. Lett., **100**, 117401 (2008).
- [21] R. R. Nair, P. Blake, A. N. Grigorenko, K. S. Novoselov, T. J. Booth, T. Stauber, N. M. R. Peres, A. K. Geim, Science **320**, 1308 (2008).
- [22] M. Ezawa, Phys. Rev. B, **73**, 045432 (2006).